Atmos. Meas. Tech., 3, 1363–1375, 2010
www.atmos-meas-tech.net/3/1363/2010/
doi:10.5194/amt-3-1363-2010

Atmospheric Measurement Techniques

A new fully automated FTIR system for total column measurements of greenhouse gases

M. C. Geibel, C. Gerbig, and D. G. Feist

Max Planck Institute for Biogeochemistry, Hans-Knöll-Str. 10, 07745 Jena, Germany

Received: 27 June 2010 – Published in Atmos. Meas. Tech. Discuss.: 22 July 2010
Revised: 20 September 2010 – Accepted: 29 September 2010 – Published: 11 October 2010

Abstract. This article introduces a new fully automated FTIR system that is part of the Total Carbon Column Observing Network (TCCON). It will provide continuous ground-based measurements of column-averaged volume mixing ratio for CO_2, CH_4 and several other greenhouse gases in the tropics.

Housed in a 20-foot shipping container it was developed as a transportable system that could be deployed almost anywhere in the world. We describe the automation concept which relies on three autonomous subsystems and their interaction. Crucial components like a sturdy and reliable solar tracker dome are described in detail. The automation software employs a new approach relying on multiple processes, database logging and web-based remote control.

First results of total column measurements at Jena, Germany show that the instrument works well and can provide parts of the diurnal as well as seasonal cycle for CO_2. Instrument line shape measurements with an HCl cell suggest that the instrument stays well-aligned over several months.

After a short test campaign for side by side intercomaprison with an existing TCCON instrument in Australia, the system will be transported to its final destination Ascension Island.

1 Introduction

Surface flux estimations of CO_2 on regional to global scales have so far been derived by a combination of data from a global network of surface sites (GLOBALVIEW-CO2) and the results of global transport models (Gurney et al., 2002; Rayner et al., 1999; Tans et al., 1990). The main advantages of the surface measurements are that they are highly accurate and that they can be obtained with moderate effort even in remote locations. The main disadvantages are that they are stronlgy influenced by local sources and sinks and that they can only provide measurements from within the atmospheric boundary layer. Despite the high accuracy of the measurements themselves, imperfect representation of vertical mixing near the surface in atmospheric transport models still leads to large uncertainties in modelled tracer mixing ratios (Gerbig et al., 2008).

The existing in situ network can be complemented by precise and accurate total-column-averaged CO_2 volume mixing ratio (VMR) measurements – commonly referred to as X_{CO_2}. The column integral of the CO_2 VMR profile is less sensitive to diurnal variations in atmospheric boundary layer height and details of vertical transport in general (Gerbig et al., 2008). It exhibits less spatial and temporal variability than near-surface in situ data, while retaining information about surface fluxes (Gloor et al., 2000). Rayner and O'Brien (2001) have shown that globally distributed X_{CO_2} measurements with an accuracy in the range of $\pm$ 1.5–2.5 ppmv would be effective in constraining global-scale carbon budgets. However, such X_{CO_2} measurements are still very sparse.

Recent analyses of solar spectra obtained by near-infrared Fourier Transform Spectrometers (FTIR) demonstrate that X_{CO_2} can be retrieved with high precision (Messerschmidt et al., 2010; Washenfelder et al., 2006; Warneke et al., 2005; Dufour et al., 2004; Yang et al., 2002). These measurements make use of characteristic absorption lines that many atmospheric trace gases exhibit in the infrared region of the electromagnetic spectrum. From the difference of the known solar spectrum from space and the measured solar spectrum after passing through the atmosphere, the total column of gases like CO_2, CH_4 and many others can be calculated. To obtain the column-averaged volume mixing ratio, these values have to be divided by the total dry air column. The total dry air column can be derived either from surface pressure or from the

Correspondence to: M. C. Geibel
(mgeibel@bgc-jena.mpg.de)

measured O_2 total column (for details see Eqs. 1–3). Unlike surface measurements, the total column measurements provided by ground-based FTIR instruments can also be used directly for the validation of satellite instruments like GOSAT (Yokota et al., 2009).

The Atmospheric Remote Sensing group (ARS) of the Max Planck Institute for Biogeochemistry (MPI-BGC) in Jena, Germany, is currently making the final preparations for installing such an FTIR instrument in the tropics, where such measurements are very sparse. So far the only tropical TCCON site is Darwin, Australia (Deutscher et al., 2010). Other measurements have only been taken during short campaigns (Petersen et al., 2010; Warneke et al., 2010). The instrument will be part of the Total Carbon Column Observation Network (TCCON) (Wunch et al., 2010; Toon et al., 2009) that provides ground-truth data for satellite validation. It will be installed on Ascension Island, a British oversea territory in the South Atlantic. This unique location should provide excellent observation conditions for the FTIR instrument. Due to its small size and very scarce vegetation, the influence from local sources and sinks on the CO_2 and CH_4 measurements should be minimal.

The instrument has been set up and tested at the MPI-BGC in Jena, Germany. This article provides a technical overview of the system and shows first results obtained during this initial phase.

2 The MPI-BGC FTIR system

Most existing FTIR systems were usually built for one special location and designed to cope with that location's typical special environmental conditions. Several of those systems are automated or can at least be controlled remotely through a data connection. Exceeding these capabilities, the main goal of the MPI-BGC's FTIR project was to build an instrument that could be deployed nearly anywhere in the world (Fig. 1). It should be easily transportable by truck, train or ship. In addition to that, two persons should be able to set it up at a new location within one week. After setup, no manpower should be required during regular operation for at least six months.

However, building such a system is challenging. In a remote region with little infrastructure to rely on such an instrument has to be able to run fully automatic without operator intervention for months or even years. This challenge added several problems that had to be solved in addition to setting up the instrument itself. All components had to be designed or modified to minimize the risk of technical failures or software errors. Wherever possible, key devices were simplified to avoid problems arising from unnecessary complexity. Essential devices were set up redundantly to provide essential functions even in the case of a failure.

The components have been chosen on the basis of reliability, stability and maintainability. All of them are grouped into three autonomous modules – each of them designed to perform special tasks in the system as reliably as possible in the most simple way. These modules are the weather station, the Programmable Logic Controller (PLC) and the Master PC. A star-shaped automation concept where all components are controlled by a single master system would also have created a potential single point of failure. Therefore the three autonomous modules were set up so that they are able to check each other's performance or even reset each other in the case of a failure. Detailed information can be found in Sects. 2.4 and 2.5.

Fig. 1. Picture of the MPI-BGC FTIR container at its preliminary location close to the MPI-BGC in Jena.

2.1 The container

One of the main targets was to create a system that is relatively easy to transport. Therefore, the system is housed in a custom-made 20-foot shipping container made by CHS CONTAINER GmbH Bremen, Germany (see Figs. 1 and 2). It is equipped with enhanced insulation and has a fully integrated air conditioning system consisting of a Stulz CCU 81A (STULZ GmbH, Germany), a Guentner S-GVV047C/CW heat exchanger (Guenther Kaelte-Klima GmbH, Germany) and in adition a Remko EFT 240 dehumidifier (REMKO GmbH & Co. KG; Germany). This provides stable indoor operating conditions at outdoor temperatures from −40 °C to +40 °C.

The container is fully certified for land as well as ship transport and can be transported like any standard freight container. This offers high flexibility at reasonable shipping prizes. Besides stable inside environmental conditions, stable electric power is essential for operation. The system requires 3-phase AC with 400 V/32 A/50 Hz and has an average power consumption of 1–3 kW (site-dependent, max. peak 10 kW). An uninterruptible power supply (UPS, MGE UPS Comet EX RT, 7 kVA) is integrated to bridge power failures

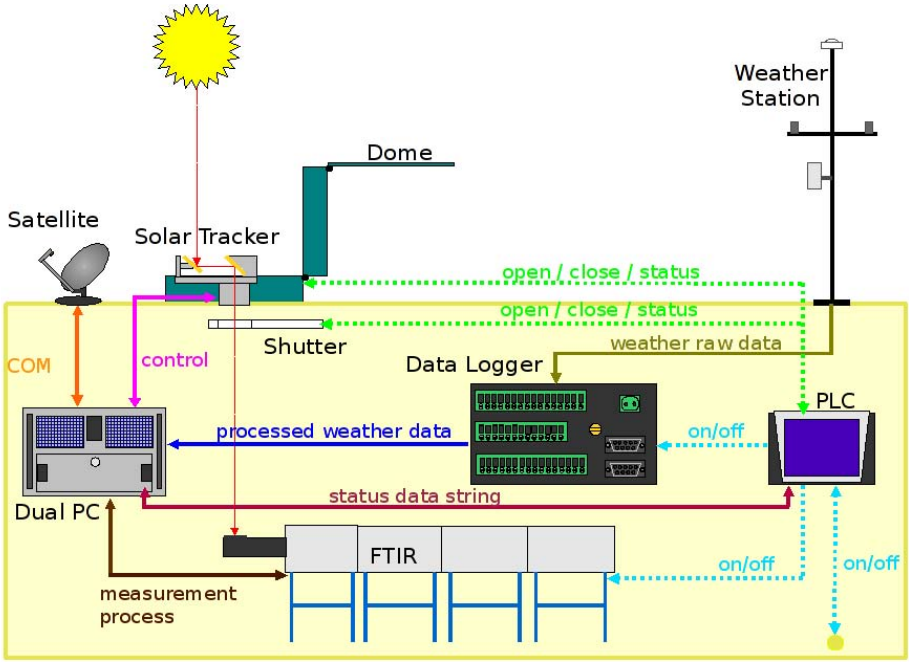

Fig. 2. Schematic overview of the MPI-BGC FTIR system. It illustrates all major parts of the system. The communication flow between the individual components is indicated by arrows.

of up to two hours. The focus transportability continues with the components: Nearly all items inside of the container are intigrated in transport-ready state. All items mounted on the roof have their defined transport location inside the container. All of the roof-mounted items are constructed in a way that they can be lifted just with the help of a pulley (see Fig. 1). No additional utilities like cranes are needed.

2.2 Fourier Transform Infrared Spectrometer (FTIR)

The atmospheric measurements are performed by a Bruker 125HR FTIR instrument. The instrument provides high resolution solar absorption spectra over a large spectral range. The resolution of the instrument is 0.0035 cm^{-1} and it covers a bandwidth from 3800 cm^{-1} to 15 800 cm^{-1} with the current detectors. Similar to the Park Falls instrument (Washenfelder et al., 2006) it is equipped with two detectors measuring simultaneously in different spectral ranges. A silicon diode detector covers the spectral range from 9000 cm^{-1} to 15 800 cm^{-1}. An Indium-Gallium-Arsenide (InGaAs) detector covers the spectral range from 3800 cm^{-1} to 12 000 cm^{-1}.

To enhance the stability of the system and avoid spectral contamination by water vapor, all measurements are performed under vacuum. Therefore the system is equipped with a multi-stage oil-free scroll pump (Varian TriSrcoll300). To avoid vibrations of the pump influencing the measurements, the pump only runs during night time.

For accurate measurements the monitoring of the instrumental line shape is necessary. This is realized as described by Hase et al. (1999) by integrating an HCl gas cell (length 10 cm, diameter 4 cm, filling pressure 5.013 mbar) in the beam path inside the FTIR instrument. It is located directly in front of the 1st aperture. First results of this procedure are described in Sect. 3.1.

The atmospheric measurements are performed with the same settings that were used by Messerschmidt et al. (2010): a 0.014 cm^{-1} resolution (corresponds to an optical path difference of 65 cm) with an aperture of 1 mm diameter and a scanner velocity of 10 kHz. The electronic low pass filter is set to 10 kHz (corresponds to 15 798 cm^{-1}). The high folding limit for the Fourier transformation to 15 798 cm^{-1}. Two individual scans, one forward and one backward, are made per measurement.

2.3 Solar tracker and protective devices

Remote sensing of greenhouse gases via FTIR uses the sun as a light source. The container has an open flange in the roof. Mounted on top of this is a Bruker Solar Tracker type A547 (see Fig. 3). It is controlled by its own PC (see Sect. 2.4.3) and follows the sun and guides the sunlight into the container. The flange and the tracker have to be protected from bad weather such as rain, snow and high wind speed. Therefore a special dome was developed.

Fig. 3. The Bruker Solar Tracker type A547 mounted in the custom made dome (shown in open state).

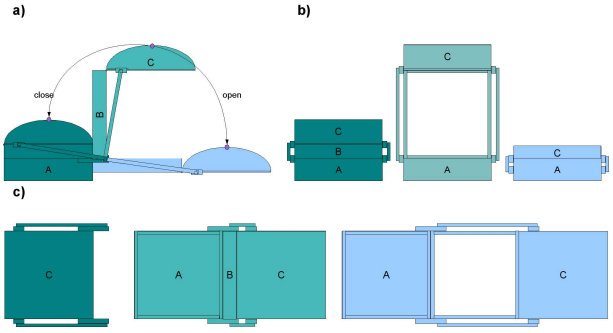

Fig. 4. Schematic overview of the BGC-FTIR Solar Tracker Dome in side **(a)**, front **(b)** and top view **(c)**. Equal colours represent equal states of the dome. The dome consists of a frame of aluminum x-profile beams that are covered with aluminum plates. Its z-shaped movement is realized by two arrays of hinges and a moving lever. The middle part (Part B) is an open frame. The upper part (Part C) of the lid always faces upwards.

2.3.1 The solar tracker dome

The dome for the solar tracker is a crucial part of the system. It has to meet several demands. In the closed state it should be small but still allow the tracker to move into every position. It has to protect the tracker and the flange beneath from rain, snow and hail as well as strong winds and flying debris. In the open state it should allow the tracker an unobstructed 360° view. The mechanism has to be simple and reliable.

Our solution to these demands consists of a frame of aluminum x-profile beams that are covered with aluminum plates. Its z-shaped movement (see Fig. 4) is realized by two arrays of hinges and a moving lever. This lever is powered by a gear motor via a tooth-belt drive.

The middle part (Part B in Fig. 4) was constructed as an open frame. Therefore the area exposed to the wind does not increase during the opening or closing process. This way, even high wind speeds do not inhibit the movement of the dome. This ensures that it can be closed under all conditions. Also note that the upper part of the lid always faces upwards. This way the tracker cannot be harmed by water, dirt or other objects (leafs etc.) that may have collected in the open lid when the dome is closed.

2.3.2 The shutter

A failure of the dome mechanism cannot be ruled out completely. Therefore, an additional shutter was constructed as a backup mechanism to close the container even in case the dome should fail. The shutter also provides additional thermal insulation between the container and the dome. This saves energy and avoids condensation problems when the dome is closed.

The shutter basically works like a drawer and is mounted on the ceiling directly underneath the flange (Fig. 2). Usually it is opened and closed simultaneously with the dome but can be operated independently if necessary. The main part is a polyamide block with a hole on one and a drain on the other side. It slides via four ball bearings on two polished steel rails. The shutter is moved by a spindle-motor and the accurate positioning is realized with two limit switches. In the open position, the hole in the shutter is congruent with the hole in the flange. This way the sun light can travel from the tracker down into the spectrometer.

When the shutter is closed, the drain slides under the hole in the flange and seals the container. In case of a dome failure, rain is collected by the drain and guided into a reservoir.

2.4 Hardware components for automation

For the automation the system was divided in three autonomous modules. Each of these modules is designed to be as reliable as possible. In case of a malfunction or a complete failure of a component, the modules bring the system to a defined standby or sleeping state. The design goal was that any failure of a single component would not leave the system in an undefined state.

2.4.1 Weather station

The weather station (Fig. 5) is equipped with a number of different sensors to monitor outdoor and indoor conditions (Table 1). Most of the sensors are redundant since their data are either crucial for the measurement process or for the protection of the system against bad weather conditions.

Indoor as well as outdoor temperature and humidity are measured by redundant pairs of sensors. A pyranometer measures global radiation which is useful to determine appropriate measurement conditions without opening the dome. Wind speed is measured by two cup anemometers that were chosen for their reliability. Precipitation is detected by two different approaches: The first sensor works with a light barrier that can detect rain, hail and also other flying objects

Table 1. Weather station equipment.

Sensor	Position	Type
Temperature/Humidity	2 outdoor	Galltec + Mela C2.4
Temperature /Humidity	2 indoor	Campbell CS215
Temperature	2 in the FTIR	Campbell T107
Global radiation	1 outdoor	Kipp & Zonen Pyranometer CMP3
Precipitation	2 outdoor	Lambrecht Electronic 15153 & 15152
Wind speed	2 outdoor	Lambrecht Wind Sensor Industrial 14557
Ambient pressure	2 outdoor	Vaisala PTB210

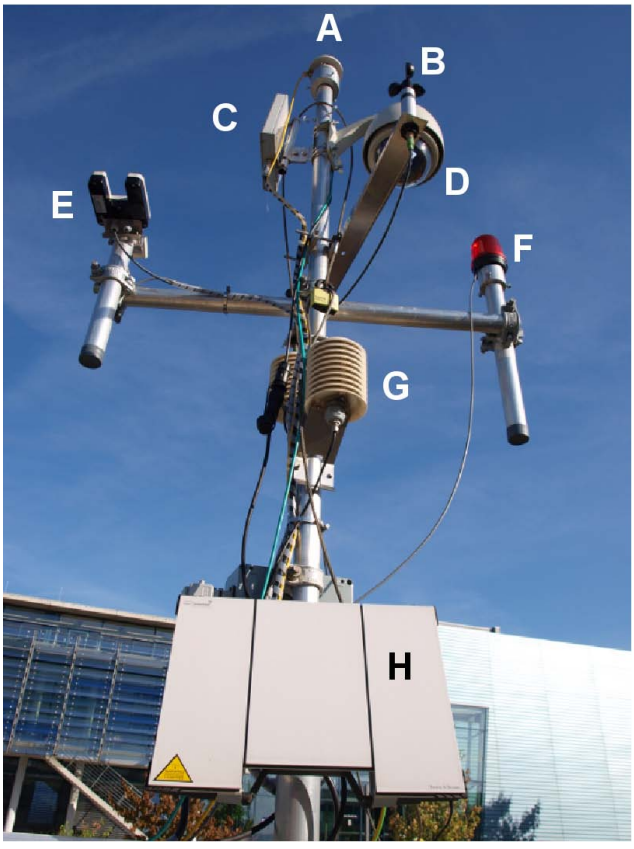

Fig. 5. The weather station mounted on top of the FTIR container. It measures temperature and humidity with two sensors (G). Wind speed is measured by two cup anemometers (B). It is also equipped with two different precipitaion detectors (E). On the very top, global radiation is measured by a pyranometer (A). The pole of the weather station also hosts two antennas for communication: a wireless LAN link (B) and a BGAN satellite receiver (H). Also an outdoor camera (D) and a signal LED (F) are mounted on the pole.

like insects. The second precipitation sensor detects changes in conductivity when it is hit by rain or snow. This one is also able to detect fine spray.

Highly accurate and stable pressure measurements are essential for the quality of the retrieved mixing ratio profiles (see Eq. 2). However, long-term drift of these sensors is a problem that cannot be avoided easily. To be able to detect and correct such a drift three highly accurate digital Vaisala PTB210 pressure sensors and a special recalibration scheme where chosen.

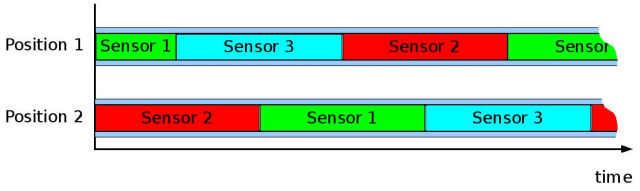

Fig. 6. Pressure sensor recalibration scheme. Sensors 1 and 2 are used for redundant measurements while sensor number 3 is a calibrated spare that replaces one of the two used sensors (e.g. sensor 1) at the next maintenance after aproximately 6 months. Sensor 1 will then be recalibrated and later replace sensor 2.

Figure 6 explains how this recalibration scheme works: Sensors 1 and 2 are used for redundant measurements while sensor number 3 is a calibrated spare. At a regular maintenance visit sensor 3 will replace one of the two used sensors (sensor 1 in this example). Sensor 1 will then be recalibrated and later replace the other sensor – in this example sensor 2 – during the next maintenance visit. This leap-frog calibration scheme allows to detect and compensate any drift of the sensors. One sensor always stays in the system as a reference. This way, a detected drift in one of the sensors can be corrected and discontinuities in the pressure measurements can be avoided. With this scheme, one should be able to maintain the original ± 0.1 hPa accuracy of the sensors over a period of many years.

The precipitation sensors are directly connected to the PLC (see Sect. 2.4.2) to ensure that dome and shutter can be closed as quickly as possible when it starts to rain. All other sensors are connected to a Campbell Scientific CR 1000 data logger. This data logger processes the raw data and makes them available to the Master PC via an ethernet connection (Fig. 7). Details of the weather station can be found in Zöphel (2008).

For the communication with the CR 1000 data logger, the software project PyPak was developed. PyPak has been released as a free software project under the GNU General Public License (available at http://pypak.sourceforge.net/).

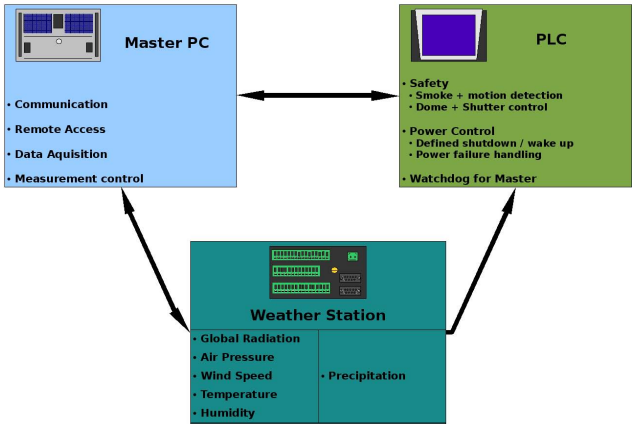

Fig. 7. Schematic overview of the communication. The three major parts of the FTIR system are autonomous systems. They communicate over a serial and an ethernet connection, repectively.

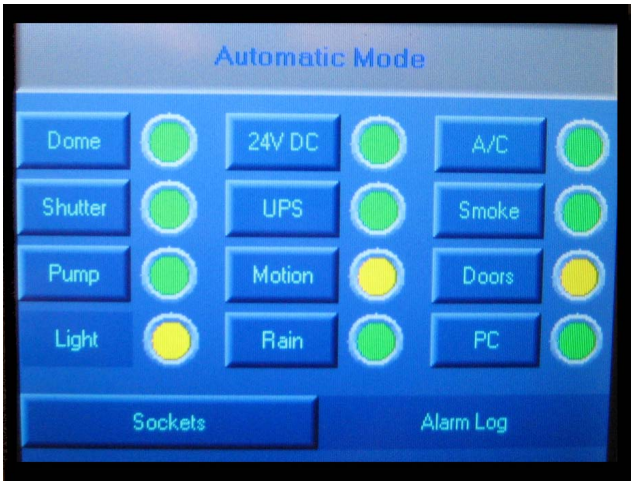

Fig. 8. PLC control panel showing the PLC operating in automatic mode. It shows the actual container status, the colored bullets indicate status of each component – whereas green stands for "OK", yellow for "in progress" and red indicates "alert". Detailed information can be accessed via the sub menus.

2.4.2 Programmable Logic Controller (PLC)

The Programmable Logic Controller (PLC, Unitronics Vision 570-57-T40B) is the backbone of the container and one of the most crucial components. Its main target is to bring the container into one of several predefined states depending on external circumstances. It also indicates this status to the Master PC and executes its requests to change this status (Fig. 7). The PLC has full control over the dome and the shutter and controls the power lines of most other components (including the Master PC). The PLC is also connected to different sensors and switches to determinate the status of many components. The communication to the Master PC is established via an RS232 connection. If the Master PC should fail to communicate with the PLC for too long, the PLC will try to restart the Master PC.

The PLC has two operational modes that can be chosen via a selector switch. The automatic mode shows the actual container status on the PLCs main screen (Fig. 8). Colored bullets indicate the status of each component: green stands for "OK", yellow for "in progress" and red indicates "alert". More detailed information can be accessed via sub menus. In this mode the PLC accepts commands only via RS232 communication. Every input command is answered by the PLC with a detailed list of the actual status of every input and output channel. Invalid commands are ignored. The status of the PLC is logged in the database on the Master PC and can so also be monitored by a remote user. In case of an emergency a direct command input with via Ethernet is possible. That way also commands of the Master PC can be overruled.

The other operation mode – the manual mode – is for manual operation during maintenance. In this mode all parts of the PLC system can be accessed and operated manually through their sub menus. External commands from the Master PC are ignored in this mode.

In case of a power failure the PLC ensures that all components are properly shut down and the dome is closed before the UPS battery runs out. It is also the first part of the system that automatically restarts after such a shutdown. All the other components are afterwards restarted in a defined cascade until the whole system is fully operational again.

2.4.3 Dual PC

For high availability, the container is equipped with an industrial 19-inch rack-mount computer system (ARBOR Technology Corp. IEC-620). The chassis includes two redundant power supplies, temperature monitoring, and a temperature controlled fan cascade. It hosts two independent Slot-CPUs in the same case (Table 2): one for the measurement process, communication and data storage (Master PC) and one for the control of the solar tracker (Tracker PC). Passively cooled low-energy CPUs were chosen to avoid a system malfunction due to a fan failure.

Master PC

The Master PC is responsible for the communication, data storage and the automation of the whole system (see Sect. 2.5). It runs a Debian Linux system that can be fully controlled remotely, even over low bandwidth links. For the other components, the Master PC also provides network-related services like routing, name service or email handling. Through the network time protocol (NTP), it also provides accurate time information from a GPS receiver to the internal network.

To the PLC and the Tracker PC, the Master PC is connected via an RS-232 serial line. All other components like

Table 2. Dual PC components.

Component	Master PC	Tracker PC
Mainboard	PCA-6004H-00A2E Advantec	PCA-6002VE-00B1E Advantec
CPU	VIA C3 800MHz	Intel Celeron Tualatin 400 MHz
RAM	1024 MB	128 MB
Additional Cards	SCSI, Serial	Bruker Solar Tracker Controller Card
Diskspace	Infotrend EonStor SCSI RAID ES U12U-G4020M2 12×72 GB	1 GB SSD Compact Flash
Storage	HP StorageWorks DAT 72×10 10x auto loader	

the spectrometer, the UPS, the weather station data logger, internal and external cameras are accessed over the internal network (Fig. 7).

Data is stored on a high-availability RAID system with redundant power supplies. In the current configuration it hosts twelve SCSI hard disks of 72 GB each. The total usable disk space in the current configuration is 280 GB with four redundant disks and four spare disks. The maximum configurable redundant disk space would be 792 GB with no spares. Disk configurations can be changed – even remotely – while the system is operating.

In addition to the disk, data can also be stored on a tape drive (HP StorageWorks DAT 72×10 auto loader). It has a maximum capacity of ten DDS-5 tapes with an uncompressed capacity of 36 GB each. The tapes were chosen for their small form factor which makes it easy to send them by post.

Tracker PC

For improved reliablility, the Tracker PC is a fan-less and disk-less system that needs only low performance. Data is stored on a flash memory card. The operating system is a minimal Debian Linux which emulates a FreeDOS environment for the original solar tracker software. This way, the solar tracker software can be controlled over the network and the clock can be synchronized through NTP.

2.5 Automation concept

2.5.1 Communication, data storage and transfer

The container can be accessed remotely in two ways. First, it has a wireless link that can cover up to 2 km to the next available internet access. It also is equipped with an Inmarsat BGAN satellite receiver (Thrane & Thrane Explorer 700) that provides a high-speed internet connection almost anywhere in the world. However, the transfer of large amounts of data over the satellite link is very expensive, so this link is intended mostly for remote control.

If there is no alternative internet connection, data can also be saved to DDS-5 (DAT) tapes with an uncompressed capacity of 36-GB. The tape drive can hold up to ten tapes. Due to their small form factor and weight, these tapes can be mailed easily.

2.5.2 Software

The concept for the automation software, which is displayed in Fig. 9, reflects the modular design of the hardware components. Each main hardware module (PLC, solar tracker, weather station) has an independent background process – a so-called daemon – that handles communication with the respective module. The daemons are started at system boot and are restarted automatically if they should exit prematurely.

Each daemon communicates continuously with its hardware module. The daemons log status information or data from the weather station at regular intervals. The PLC and the solar tracker daemon can also receive commands through a TCP/IP socket. These commands are then forwarded to the PLC or solar tracker, for example to open or close the solar tracker dome or change the solar tracker operation mode.

All status information is logged in a central MySQL database. A database approach was chosen over file-based logging because it is safer and offers much more flexibility. For example, the MySQL server makes sure that data can be read and written simultaneously by several processes. It is also easy to search for data or retrieve it in a different format then the one it was written. Mirroring the whole database to another MySQL server over the internet is also straightforward.

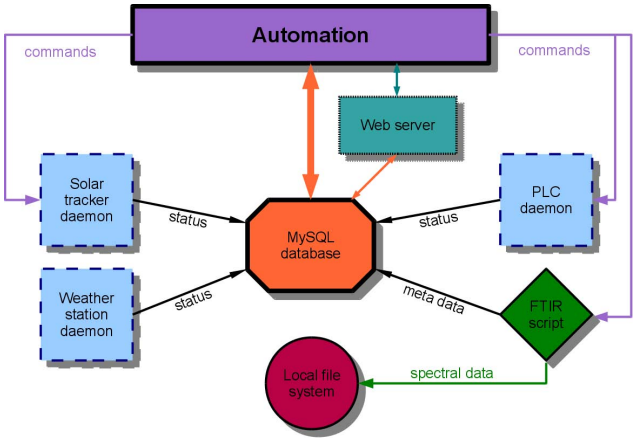

Fig. 9. Schematic overview of the automation software components.

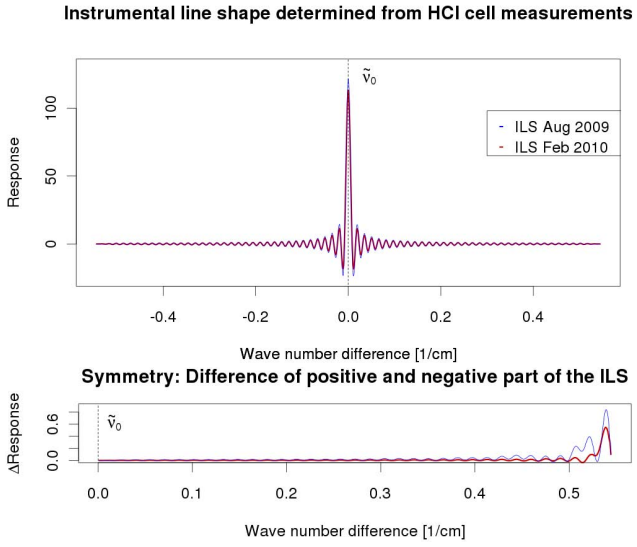

Fig. 10. Comparison of the instrument line shape of the Jena Bruker IFS125HR in August 2009 and February 2010. The x-axes represent the wavenumber difference relative to the center peak position $\tilde{\nu}_0$. The lower part of this Figure shows the difference between the positive and negative part of the ILS as a measure of symmetry.

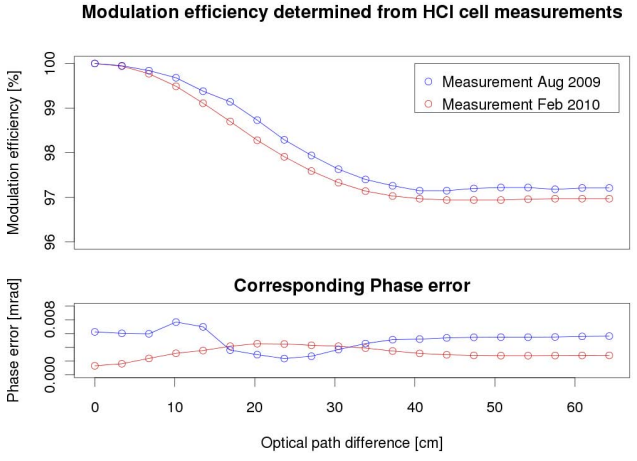

Fig. 11. Changes in the modulation efficiency and phase error of the Jena BRUKER IFS125HR from August 2009 to February 2010.

The automation module is also a daemon. It uses a list of rules to translate the detailed log information from the database into more abstract system states. For example, one system state is that the system is sleeping during the night or that it is ready to start a measurement. Important: the rules themselves are not part of the program. Instead, they are also defined in the database and can be changed any time. There is no need to change the software if the automation rules have to be adapted.

Measurements are started by the automation daemon whenever all necessary pre-conditions have been met. The FTIR measurement script runs once and exits after the measurement. While it runs, it logs its actions to the database. The spectral data is saved in files on the local file system.

The whole system is controlled by daemon processes that do not provide a user interface. To monitor the activity of the FTIR container remotely, a web server displays the information from the database in a user-friendly way. Through the web interface, it is also possible to change the automation rules or control other parts of the FTIR container.

3 First results

3.1 Alignment

For the accurate retrieval of total column values, a good alignment of the FTIR is crucial. The instrument line shape (ILS) is retrieved from HCl cell measurements is a useful indicator of the FTIR's alignment (Hase et al., 1999). The performed measurements were analyzed with the Linefit spectrum fitting algorithm (Hase, 2010).

Figures 10 and 11 show the results of an ILS retrieval from HCl cell measurements from August 2009 and February 2010. The modulation efficiency decreased slightly during these six months (see Fig. 11). Nevertheless, the maximum loss in modulation efficency is 3%. For comparison other well aligned TCCON intruments reach values for modulation efficency of better then 95%. The phase error for both measurements is well below 0.01 rad which Hase et al. (1999) considered as a good value.

Figure 10 illustrates the symmetry of the ILS. The top plot shows both ILS measurements plotted over the difference of the wavenumber $\tilde{\nu}$ and the center peak wavenumber $\tilde{\nu}_0$ (Griffiths and de Haseth, 1986). The lower plot shows the difference of the positive part ($\tilde{\nu} > \tilde{\nu}_0$) and the negative part ($\tilde{\nu} < \tilde{\nu}_0$) as a measure of symmetry. The observed deviations from symmetry are very small as one should expect from a well-aligned FTIR.

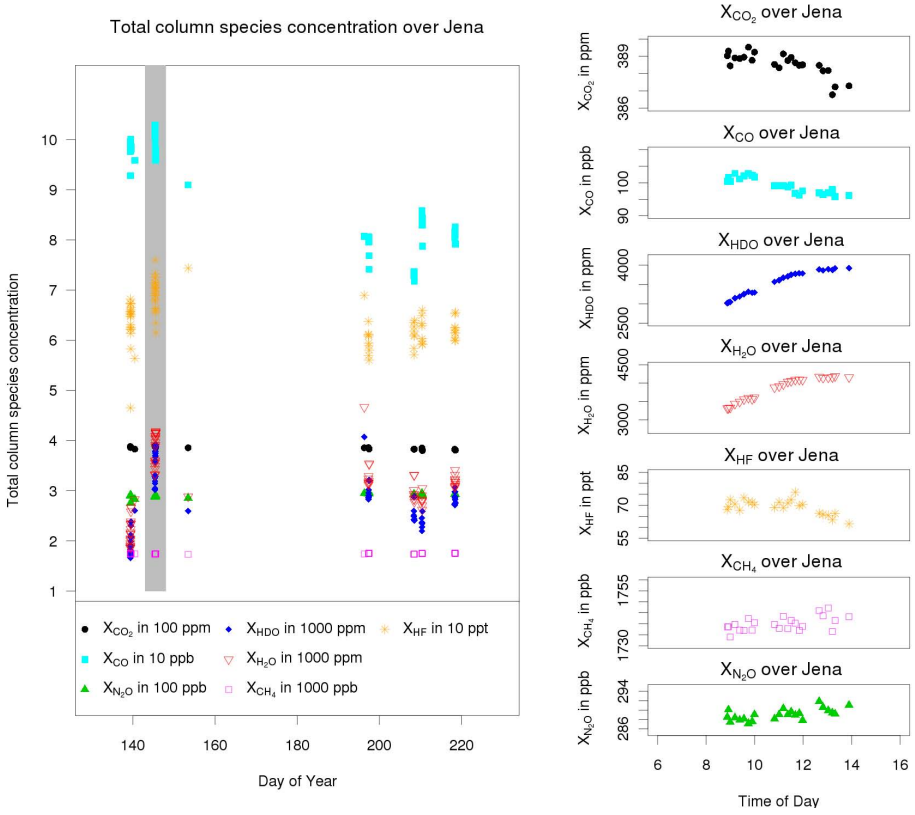

Fig. 12. Standard TCCON anaysis of measurements taken with Jena FTS 2009. The right column of plots show the diurnal variation of the species for the day marked in the left plot.

3.2 Column measurements at Jena

In 2009 measurements were taken during the setup of the instrument and the automation of the system. Due to the ongoing construction, the time series is relatively sparse. The site is located at the outskirts of Jena, Germany, at 50.910° N, 11.569° E, 211 m a.s.l. (above sea level).

The acquired data was processed with TCCON standard analysis software GGG (Wunch et al., 2010). GGG is a suite of software tools developed at Jet Propulsion Laboratory (JPL) to determine the abundances of atmospheric trace gases from infrared solar absorption spectra. This software evolved from the ODS software (Norton and Rinsland, 1991) used for the Version 2 analysis of ATMOS data, but has incorporated many improvements since then. The most complex program in the GGG suite is GFIT, the spectral fitting code. GFIT has been used for the analysis of MkIV spectra (balloon, aircraft, and ground-based), plus the Version 3 analysis of ATMOS shuttle spectra (Irion et al., 2002). Also GFIT has been used for the analysis of spectra from several ground-based FTIR spectrometers (Notholt et al., 1997). In recent years GFIT and has become the standard data analysis tool for TCCON. The number of species retrieved from GFIT and the associated number of analyzed micro windows after TCCON specifications can be found in Table 3. An overview of the retrieved species from the measurements in Jena can be found in Fig. 12.

As described in Wunch et al. (2010), CO_2 is retrieved in the 6220 cm^{-1} and 6339 cm^{-1} micro windows, O_2 in the 7885 cm^{-1} micro window, CH_4 in the 5938 cm^{-1}, 6002 cm^{-1} and 6076 cm^{-1} micro windows and CO in the 4233 cm^{-1} and 4290 cm^{-1} micro windows. The dry air column-averaged mole fractions are calculated from the gas columns (Γ), according to

$$f_{\mathrm{CO_2,\ avg}} = \frac{\Gamma_{\mathrm{CO_2}}}{\Gamma_{\mathrm{dry\ air}}} \tag{1}$$

As shown by Washenfelder et al. (2006), there are two methods for calculating the total dry air column $\Gamma_{\mathrm{dry\ air}}$. Both methods have specific advantages and disadvantages:

$$\Gamma_{\mathrm{dry\ air,\ P}} = \frac{P_{\mathrm{S}}}{m_{\mathrm{air}} g} - \Gamma_{\mathrm{H_2O}} \tag{2}$$

with m_{air} – air mass, P_{S} – surface pressure, g – gravity constant

$$\Gamma_{\mathrm{dry\ air,\ O_2}} = \frac{\Gamma_{\mathrm{O_2}}}{0.2095} \tag{3}$$

In general the approach of calculating the total dry column via surface pressure with Eq. (2) is more precise since

Table 3. Table of species retrieved from GFIT and the associated number of analyzed micro windows according to TCCON specifications.

Species	Micro Windows	Standard output
CH_4	3	yes
CO	2	yes
CO_2	2	yes
HF	1	yes
HCl	16	no
HDO	4	yes
H_2O	9	yes
N_2O	2	yes
O_2	1	no

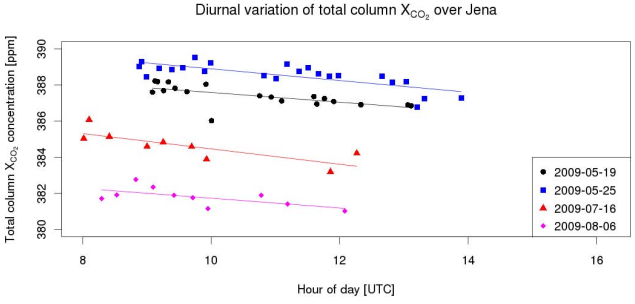

Fig. 13. Diurnal variation of total column X_{CO_2} over Jena shown on selected days. The decrease of X_{CO_2} over the day was relatively constant.

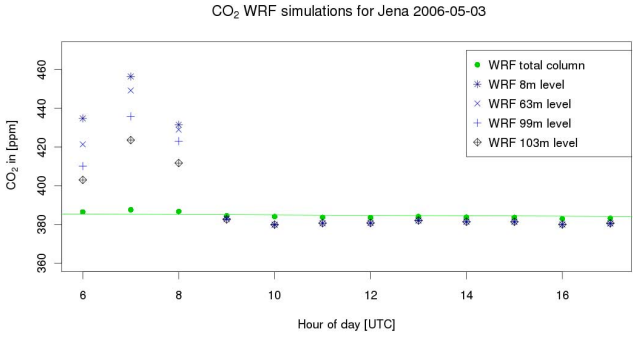

Fig. 14. Diurnal variation of CO_2 from WRF-VPRM for total column and lower levels over Jena. The model resolution is 2 km.

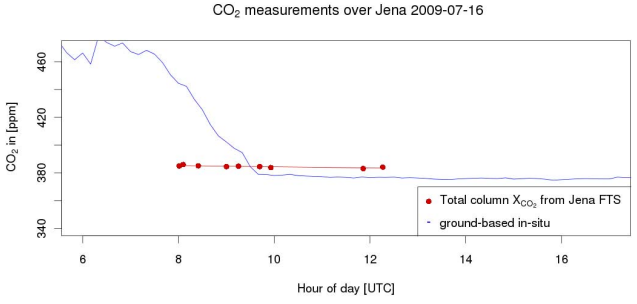

Fig. 15. Diurnal variation of ground-based in-situ CO_2 and total column X_{CO_2} over Jena. The gaps in the time series are due to clouds.

P_S can be measured very accurately (see Sect. 2.4.1). Using the more noisy retrievals of the O_2 column for the calculation in Eq. (3) will increase the random scatter. However, non-perfect measurement conditions (like pointing errors and variation of intensity during the measurement) and systematic errors will affect the O_2 and CO_2 retrievals in a similar way. Those are reduced when $\Gamma_{\text{dry air}}$, O_2 is used in Eq. (1) .

Due to ongoing construction and limited field of view, we were not able to cover full diurnal cycles. Nevertheless, the measuered diurnal variation of total column X_{CO_2} over Jena (Fig. 13) illustrates the decrease in atmospheric X_{CO_2} over the covered period in more detail. It shows also that the decrease of X_{CO_2} over the day is relatively constant.

An important feature of total column measurements is that – compared to surface measurements – they are less affected by variability induced by vertical transport and local sources and sinks. That is in fact one of the main reasons why total column measurements can complement the existing in-situ network (Rayner and O'Brien, 2001).

This insensitivity of the total column can be found in high-resolution model simulations. We analysed WRF-VPRM model data (Pillai et al., 2010) from 2006 for the Jena area. Figure 14 shows this nocturnal build-up of CO_2 in the lower levels that decreases with height. This feature was found for several days in the analysed model data. As the vertical mixing starts in the morning this build-up is quickly diluted with residual layer air. The figure also shows that the sensitivity of the calculated total column X_{CO_2} to the boundary layer effects are very small. Unfortunately, model data that cover the period of our FTIR measurements are not yet available.

Expecting similar results from measurements, we compared the total column X_{CO_2} data measured with the Jena FTIR to ground-based in-situ CO_2 measured on the roof of the MPI for Biogeochemistry. The in-situ measurements are performed with non-dispersive infrared (NDIR) gas analyzer type LI-COR LI-6262. As expected from the model analysis, the diurnal variation of X_{CO_2} next to the ground seems not to effect the column measurements (Fig. 15). The large drop of more than 80 ppm in boundary layer CO_2 was not represented in the total column measurements. This illustrates the small contribution of the boundary layer to the total column and confirms the expectations from the model data. The FTIR measurements after 10am show a relative constant offset compared to the in-situ measurements.

Figure 16 shows the comparison total column X_{CO_2} daily averages vs. total column values calculated from TM3 inversions (Rödenbeck, 2005). Unfortunately, TM3 result were only available until the end of 2007. To compare them with the FTIR results, the TM3 results were extrapolated to 2009. For this extrapolation, the yearly cycles of 1996 till 2007

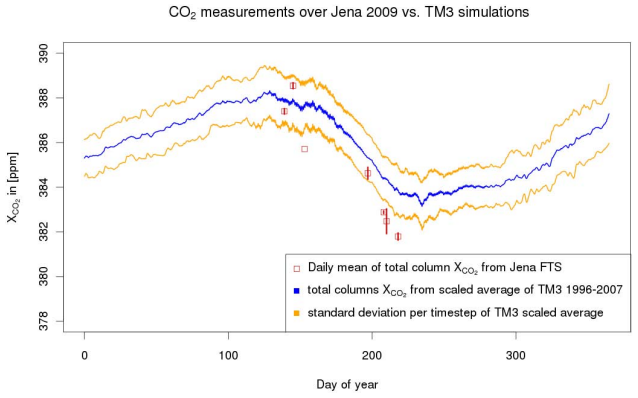

Fig. 16. Total column X_{CO_2} measurements over Jena vs. extrapolated TM3 results for 2009. Empty red boxes represent individual X_{CO_2} measurements from the FTIR. Red boxes with vertical lines represent daily mean values of X_{CO_2} with error bars (vertical lines).

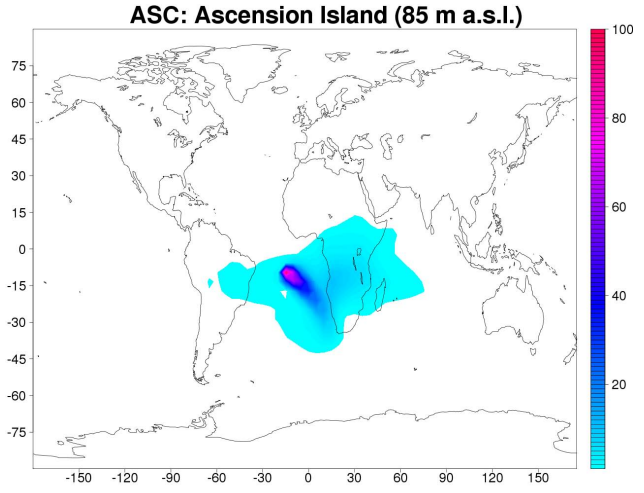

Fig. 17. Footprint analysis for a total-column instrument on Ascension Island. The coloured values represent the relative contribution to the total column for different surface regions in arbitrary units that have been normalized to 100 at the peak value. The footprint was produced using the TM3 adjoint by Rödenbeck (2005) at a horizontal resolution of $5° \times 3.75°$. Individual runs for each month of 2006 were integrated to provide this full-year footprint.

were averaged and scaled to the 2007 mean. This reduced the synoptic variability. The mean yearly cycle was then shifted for the annual mean CO_2 growth rate for the years 2008 (1.80 ppm) and 2009 (1.64 ppm) (Tans, 2010) by adding an offset of +3.44 ppm. The red empty boxes represent X_{CO_2} measured by the FTIR. respectively the daily mean (for day where more then one measurement could be performed). The vertical red lines represent the standard error of the mean value. The FTIR total column X_{CO_2} values represent the prognosted yearly cycle of 2009 well and are within respectivly close to the $1\,\sigma$ threshold.

4 Conclusions and outlook

This article describes the principal components and the design concept of the MPI-BGC FTIR system. The main design goals were reliability and low maintenance effort for operation at remote sites. This was realized through the interaction of independent subsystems that were kept as simple as possible. Critical components are redundant as much as possible.

The instrumental line shape of the FTIR was determined from HCl cell measurements. During a period of six months this ILS changed only slightly. From these results one can expect that – once aligned – the instrument will be very stable over long time persiods.

During the installation phase at Jena, Germany, the instrument measured column-averaged X_{CO_2}, X_{CO} and X_{CH_4}. Compared to ground-based in-situ CO_2 VMR measurements, the FTIR total column X_{CO_2} showed an expected offset in the morning which mostly disappeared with the breakup of the nighttime planetary boundary layer. This effect demonstrated the reduced sensitivity of X_{CO_2} measurements to mixing processes in the planetary boundary layer and confirms results of model simulations. Otherwise, the X_{CO_2} measurements show a distinct diurnal cycle. A part of seasonal cycle measured over Jena during the installation phase corresponded to TM3 simulation results that were extrapolated to 2009 values.

In September/October 2009 the MPI-BGC FTIR system and five other European FTIR stations took part in the IMECC aircraft campaign. The goal of this campaign was to determine a calibration factor between total column values calculated from in-situ aircraft profiles of CO_2, CH_4, and CO and corresponding total column values retrieved from ground-based FTIR. The results from this campaign will be published separately in the near future.

The FTIR will first take part in a test campaign to Wollongong, Australia, from June to October 2010. This campaign will provide a rare opportunity of a side-by-side intercomparison of two TCCON-type FTIR instruments on the Southern Hemisphere.

After the campaign, the instrument will be shipped to Ascension Island (7.93° S, 14.37° W) to commence long-term measurements. From this unique location it will provide the first long time series of X_{CO_2}, X_{CH_4} and other column-averaged greenhouse gases in the tropical Western Hemisphere. Ascension Island was selected because it frequently receives air masses from the rain forest regions of Africa and occasionally also from South America. Figure 17 shows a one-year footprint for the total column measurements expected from Ascension Island. Due to the small size of the island, it would also provide a rare opportunity to validate sunglint measurements by satellites. A long-term time series of flask measurements from Ascension Island already exists and other groups will provide valuable continuous in-situ surface measurements of CO_2 and CH_4 in the near future.

Acknowledgements. We would like to thank many people who have contributed to this project: the mechanical and electronic workshop of the MPI-BGC for their support, Frank Hase (IMK-FZK) for his help with the ILS analysis, all members of the Total Carbon Column Observation Network (TCCON) for their fruitful colaboration, Christian Rödenbeck for his TM3 data, and Dhanyalekshmi Pillai for her WRF-VPRM simulations.

We wish to thank the Max Planck Society for funding the FTIR instrument and the container. The publication charges for this article were covered by a special agreement between the Max Planck Society and Copernicus Publications.

The service charges for this open access publication have been covered by the Max Planck Society.

Edited by: M. Weber

References

Deutscher, N. M., Griffith, D. W. T., Bryant, G. W., Wennberg, P. O., Toon, G. C., Washenfelder, R. A., Keppel-Aleks, G., Wunch, D., Yavin, Y., Allen, N. T., Blavier, J.-F., Jimnez, R., Daube, B. C., Bright, A. V., Matross, D. M., Wofsy, S. C., and Park, S.: Total column CO_2 measurements at Darwin, Australia - site description and calibration against in situ aircraft profiles, Atmos. Meas. Tech., 3, 947–958, doi:10.5194/amt-3-947-2010, 2010.

Dufour, E., Bréon, F.-M., and Peylin, P.: CO_2 column averaged mixing ratio from inversion of ground-based solar spectra, J. Geophys. Res., 109, D09304, doi:10.1029/2003JD004469, 2004.

Gerbig, C., Körner, S., and Lin, J. C.: Vertical mixing in atmospheric tracer transport models: error characterization and propagation, Atmos. Chem. Phys., 8, 591–602, doi:10.5194/acp-8-591-2008, 2008.

GLOBALVIEW-CO2: Cooperative Atmospheric Data Integration Project – Carbon Dioxide. CD-ROM, NOAA ESRL, ftp://ftp.cmdl.noaa.gov/ccg/co2/GLOBALVIEW, last access: 20 September 2010, Boulder, Colorado, 2009.

Gloor, M., Fan, S.-M., Pacala, S., and Sarmiento, J.: Optimal sampling of the atmosphere for purpose of inverse modeling: A model study, Global Biogeochem. Cy., 14, 407–428, doi:10.1029/1999GB900052, 2000.

Griffiths, P. R. and de Haseth, J. A.: Fourier Transform Infrared Spectrometry, Wiley-Interschience, 1986.

Gurney, K. R., Rachel, M., Law, A. S. D., Rayner, P. J., Baker, D., Bousquet, P., Bruhwiler, L., Chen, Y.-H., Ciais, P., Fan, S., Fung, I. Y., Gloor, M., Heimann, M., Higuchi, K., John, J., Maki, T., Maksyutov, S., Masarie, K., Peylin, P., Prather, M., Pak, B. C., Randerson, J., Sarmiento, J., Taguchi, S., Takahashi, T., and Yuen, C.-W.: Towards robust regional estimates of CO_2 sources and sinks using atmospheric transport models, Nature, 415, 626–630, doi:10.1038/415626a, 2002.

Hase, F.: Linefit spectrum fitting algorithm, http://www-imk.fzk.de/asf/ftir/linefit.htm, last access: 20 September, 2010.

Hase, F., Blumenstock, T., and Paton-Walsh, C.: Analysis of the instrumental line shape of high-resolution Fourier Transform IR spectrometers with gas cell measurements and new retrieval software, Appl. Optics, 38, 3417–3422, doi:10.1364/AO.38.003417, 1999.

Irion, F. W., Gunson, M. R., Toon, G. C., Chang, A. Y., Eldering, A., Mahieu, E., Manney, G. L., Michelsen, H. A., Moyer, E. J., Newchurch, M. J., Osterman, G. B., Rinsland, C. P., Salawitch, R. J., Sen, B., Yung, Y. L., and Zander, R.: Atmospheric Trace Molecule Spectroscopy (ATMOS) Experiment Version 3 data retrievals, Appl. Optics, 41, 6968–6979, doi:10.1364/AO.41.006968, 2002.

Messerschmidt, J., Macatangay, R., Notholt, J., Petri, C., Warneke, T., and Weinzierl, C.: Side by side measurements of CO_2 by ground-based Fourier transform spectrometry (FTS), Tellus B, in press, doi:10.1111/j.1600-0889.2010.00491.x, 2010.

Norton, R. H. and Rinsland, C. P.: ATMOS data processing and science analysis methods, Appl. Optics, 30, 389–400, doi:10.1364/AO.30.000389, 1991.

Notholt, J., Toon, G., Stordal, F., Solberg, S., Schmidbauer, N., Becker, E., Meier, A., and Sen, B.: Seasonal variations of atmospheric trace gases in the high Arctic at 79° N, J. Geophys. Res., 102, 12855–12861, doi:10.1029/97JD00337, 1997.

Petersen, A. K., Warneke, T., Frankenberg, C., Bergamaschi, P., Gerbig, C., Notholt, J., Buchwitz, M., Schneising, O., and Schrems, O.: First ground-based FTIR observations of methane in the inner tropics over several years, Atmos. Chem. Phys., 10, 7231–7239, doi:10.5194/acp-10-7231-2010, 2010.

Pillai, D., Gerbig, C., Marshall, J., Ahmadov, R., Kretschmer, R., Koch, T., and Karstens, U.: High resolution modeling of CO_2 over Europe: implications for representation errors of satellite retrievals, Atmos. Chem. Phys., 10, 83–94, doi:10.5194/acp-10-83-2010, 2010.

Rayner, P. J. and O'Brien, D. M.: The utility of remotely sensed CO_2 concentration data in surface source inversions, Geophys. Res. Lett., 28, 175–178, doi:10.1029/2000GL011912, 2001.

Rayner, P. J., Enting, I. G., Francey, R. J., and Langenfelds, R.: Reconstructing the recent carbon cycle from atmospheric CO_2, $\delta^{13}C$ and O_2/N_2 observations, Tellus B, 51, 213–232, doi:10.1034/j.1600-0889.1999.t01-1-00008.x, 1999.

Rödenbeck, C.: Estimating CO_2 sources and sinks from atmospheric mixing ratio measurements using a global inversion of atmospheric transport, Tech. Rep. 6, Max Planck Institute for Biogeochemistry, Jena, Germany, http://www.bgc-jena.mpg.de/mpg/websiteBiogeochemie/Publikationen/Technical_Reports/tech_report6.pdf, last access: 20 September 2010, 2005.

Tans, P.: NOAA/ESRL: Trends in Atmospheric Carbon Dioxide, http://www.esrl.noaa.gov/gmd/ccgg/trends, last access: 20 September, 2010.

Tans, P. P., Fung, I. Y., and Takahashi, T.: Observational constraints on the global atmospheric CO_2 budget, Science, 247, 1431–1438, doi:10.1126/science.247.4949.1431, 1990.

Toon, G., Blavier, J.-F., Washenfelder, R., Wunch, D., Keppel-Aleks, G., Wennberg, P., Connor, B., Sherlock, V., Griffith, D., Deutscher, N., and Notholt, J.: Total Column Carbon Observing Network (TCCON), in: Fourier Transform Spectroscopy, OSA Technical Digest (CD), p. paper JMA3, Optical Society of America, http://www.opticsinfobase.org/abstract.cfm?uri=FTS-2009-JMA3, last access: 20 September 2010, Vancouver, Canada, 2009.

Warneke, T., Yang, Z., Olsen, S., Körner, S., Notholt, J., Toon, G. C., Velazco, V., Schulz, A., and Schrems, O.: Seasonal and latitudinal variations of column averaged volume-mixing ratios

of atmospheric CO_2, Geophys. Res. Lett., 32, L03808, doi: 10.1029/2004GL021597, 2005.

Warneke, T., Petersen, A. K., Gerbig, C., Jordan, A., Rödenbeck, C., Rothe, M., Macatangay, R., Notholt, J., and Schrems, O.: Co-located column and in situ measurements of CO_2 in the tropics compared with model simulations, Atmos. Chem. Phys., 10, 5593–5599, doi:10.5194/acp-10-5593-2010, 2010.

Washenfelder, R. A., Toon, G. C., Blavier, J.-F., Yang, Z., Allen, N. T., Wennberg, P. O., Vay, S. A., Matross, D. M., and Daube, B. C.: Carbon dioxide column abundances at the Wisconsin Tall Tower site, J. Geophys. Res., 111, D22305, doi:10.1029/2006JD007154, 2006.

Wunch, D., Toon, G. C., Blavier, J.-F. L., Washenfelder, R., Notholt, J., Connor, B. J., Griffith, D. W. T., Sherlock, V., and Wennberg, P. O.: The Total Carbon Column Observing Network (TCCON), Philos. T. Roy. Soc. A, accepted, 2010.

Yang, Z., Toon, G. C., Margolis, J. S., and Wennberg, P. O.: Atmospheric CO_2 retrieved from ground-based IR solar spectra, Geophys. Res. Lett., 29, 1339, doi:10.1029/2001GL014537, 2002.

Yokota, T., Yoshida, Y., Eguchi, N., Ota, Y., Tanaka, T., Watanabe, H., and Maksyutov, S.: Global concentrations of CO_2 and CH_4 retrieved from GOSAT: first preliminary results, Scientific Online Letters on the Atmosphere (SOLA), 5, 160–163, doi: 10.2151/sola.2009-041, 2009.

Zöphel, H.: Test and installation of an automatic weather station to provide ground-based FTIR measurements for TCCON, Master's thesis, University of Applied Sciences, http://www.bgc-jena.mpg.de/bgc-systems/pmwiki2/uploads/PhdAmpDiplomaThesis/zoephel.pdf, last access: 20 September 2010, Jena, Germany, 2008.